Journal of Applied Mechanics and Technical Physics, Vol. 43, No. 4, pp. 519–528, 2002

INTERACTION OF SHOCK WAVES WITH A COMBINED DISCONTINUITY IN TWO-PHASE MEDIA. 2. NONEQUILIBRIUM APPROXIMATION

A. A. Zhilin and A. V. Fedorov

UDC 532.529

Interaction of a shock wave and a motionless combined discontinuity separating two two-component mixtures with different initial volume concentrations is studied on the basis of numerical simulation of unsteady processes. The calculations were performed using a modified method of "coarse particles" and a high-accuracy TVD difference scheme adapted to calculation of two-phase flows. Flow parameters determined by analytical dependences coincide with those obtained by numerical simulation at large times of the process. Upon interaction of the shock wave and the combined discontinuity, the type of the transient or reflected shock wave may coincide with or differ from the type of the incident shock wave. The possibility of existence of a pressure difference at the combined discontinuity boundary, which was earlier predicted analytically, is confirmed.

The formulation of the problem of interaction of a shock wave (SW) and a discontinuity of porosity of the mixture and the solution of this problem in the equilibrium approximation are given in [1]. We analyze the results of numerical calculations of the initial-boundary problem (1), (2) from [1], which were performed in the nonequilibrium approximation of mechanics of heterogeneous media.

NUMERICAL METHODS OF THE SOLUTION

To solve numerically the system of hyperbolic equations (1) with the initial-boundary conditions (2) from [1], we used a modified method of "coarse particles" and a high-accuracy TVD difference scheme.

Method of "Coarse Particles." The problems formulated were solved by the method of "coarse particles" of the first order of approximation [3]. The finite-difference equations for determining velocities at the intermediate layer in terms of time with allowance for the buoyancy force, the expressions for the volume concentration of the heavy component at the next time layer, and the conditions of stability can be found in [4]. In calculating flows with discontinuities, we used artificial viscosity in the form suggested in [5].

TVD Scheme. To solve the problem posed by a TVD scheme, the initial system of equations should be represented in a completely divergent form. The possibility of converting the system of equations of mechanics of heterogeneous media to a divergent form was demonstrated in [6] for equations of a model that ignores the difference in pressures of the components of the mixture. It turned out that the conservation laws for a mathematical model with allowance for the difference in pressures of the components and the changes in their volume concentrations can also be written in a divergent form:

$$\frac{\partial \rho_1}{\partial t} + \frac{\partial (\rho_1 u_1)}{\partial x} = 0, \qquad \frac{\partial \rho_2}{\partial t} + \frac{\partial (\rho_2 u_2)}{\partial x} = 0, \qquad \frac{\partial u_1}{\partial t} + \frac{\partial (u_1^2/2 + \ln |\rho_1/m_1|)}{\partial x} = \frac{F_{\mathrm{S}}}{\rho_1},$$
$$\frac{\partial (\rho_1 u_1 + \rho_2 u_2)}{\partial t} + \frac{\partial (\rho_1 u_1^2 + \rho_2 u_2^2 + P)}{\partial x} = 0, \qquad \frac{\partial (\rho_2 m_2)}{\partial t} + \frac{\partial (\rho_2 u_2 m_2)}{\partial x} = \rho_2 R. \tag{1}$$

Here $P = \rho_1 + a^2 \rho_2 + C m_2 - 1$ (the remaining notation can be found in [1]).

Institute of Theoretical and Applied Mechanics, Siberian Division, Russian Academy of Sciences, Novosibirsk 630090. Translated from Prikladnaya Mekhanika i Tekhnicheskaya Fizika, Vol. 43, No. 4, pp. 36–46, July–August, 2002. Original article submitted October 22, 2001.

0021-8944/02/4304-0519 $27.00

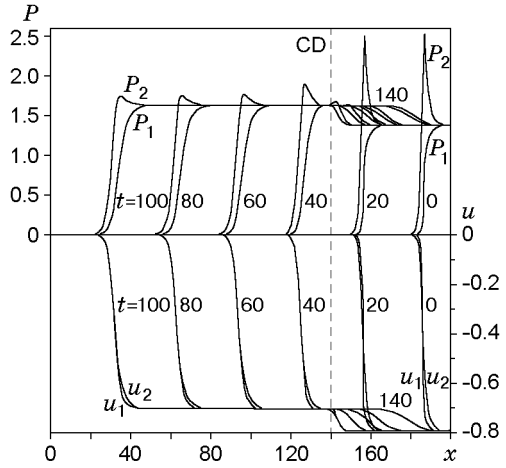

Fig. 1. Distribution of velocities and pressures of the components of the mixture upon interaction of the frozen-dispersed SW ($D = -1.5$ and $m_{10}^{*} = 0.9$) and the CD ($m_{10}^{**} = 0.7$).

Representing the initial system (1) in a vector form

$$\frac{\partial \boldsymbol{U}}{\partial t} + \frac{\partial \boldsymbol{F}}{\partial x} = \boldsymbol{G} \tag{2}$$

and finding the right and left eigenvectors of the Jacobi matrix $\partial \boldsymbol{F}(\boldsymbol{U})/\partial \boldsymbol{U} = \boldsymbol{J}$ with averaged parameters over the half-sum of values in the neighboring nodes of the grid $[\hat{x} = (x_i + x_{i+1})/2 = x_{i+1/2}]$, we use the difference analog of system (2) written in the following form in accordance with [7]:

$$\frac{\boldsymbol{U}_i^{n+1} - \boldsymbol{U}_i^n}{\Delta t} + \frac{\bar{\boldsymbol{F}}_{i+1/2}^n - \bar{\boldsymbol{F}}_{i-1/2}^n}{\Delta x} = \boldsymbol{G}_i^n.$$

Thus, the vector of the solution $\boldsymbol{U}$ at the next time layer $n+1$ is determined by an explicit formula, and the vectors of fluxes $\bar{\boldsymbol{F}}_{i+1/2}^n$ are found using the standard algorithm [7] that involves diffusion and antidiffusion terms.

The calculation results obtained by the TVD scheme and the modified method of "coarse particles" were compared with the exact solution for two types of shock-wave configurations in heterogeneous media [8, 9]. It was shown that the use of TVD schemes is more effective for solving problems of mechanics of heterogeneous media. The efficiency of the scheme was estimated by the computation time and the difference-grid step.

In calculations by the method of "coarse particles," the Courant number varied from 0.2 to 0.1. High Courant numbers correspond to continuous (dispersed) SW, and low Courant numbers refer to frozen SW [with internal and (or) bow shock waves]. In numerical calculations by the TVD scheme, the Courant number was assumed to be equal to 0.9.

DISCUSSION OF NUMERICAL RESULTS

Effect of Porosity behind the Combined Discontinuity on the Wave Pattern. We study the process of interaction of an incident SW of the frozen-dispersed type ($D = -1.5$ and $m_{10}^{*} = 0.9$) and a combined discontinuity (CD) behind which m_{10}^{**} varies from 0.7 to 0.1. For the case $m_{10}^{**} = 0.7$, Fig. 1 shows the time evolution of velocities and pressures of the components of the mixture. The dashed vertical line indicates the initial position of the CD boundary ($x = 140$). The initial SW ($t = 0$) steadily propagates over the mixture up to the CD within the time interval $t = 0$–20 and interacts with the CD, decomposing into a transient SW of the frozen-dispersed type, which continues its motion in the same direction as the incident SW, and a reflected SW of the dispersed type. The transient SW completes its formation by the time $t = 60$ and propagates with a velocity $D_{\mathrm{tr}} = -1.55$ ($t = 80$ and 100). It should be noted that the maximum pressure in the heavy phase is 2.525 before interaction with the CD and decreases to 1.748 after interaction. The final equilibrium pressure behind the incident and transient SW increases from $P_{\mathrm{fin}} = 1.384$ to $P_{\mathrm{r}} = 1.632$.

TABLE 1

Parameters of the Mixture Established after Interaction of the Incident SW ($D = -1.5$) and the CD

m_{10}^{*}	m_{10}^{**}	u_{fin}	P_{fin}	$m_{1,\text{fin}}$	u_{CD}	P_{CD}	D_{tr}	$m_{1,\text{tr}}$	D_{r}	$m_{1,\text{r}}$
0.9	0.7	−0.792	1.384	0.800	−0.704	1.632	−1.550	0.486	—	0.785
	0.5				−0.605	1.948	−1.645	0.269	0.415	0.768
	0.3				−0.515	2.252	−1.920	0.127	0.470	0.752
	0.1				−0.410	2.658	−2.533	0.033	0.533	0.732
0.5	0.9	−0.452	1.236	0.320	−0.556	0.859	−1.325	0.834	RW	0.358
	0.7				−0.505	1.035	−1.370	0.545	RW	0.339
	0.6				−0.479	1.131	−1.420	0.424	RW	0.330
	0.4				−0.422	1.353	−1.610	0.230	—	0.310
	0.3				−0.390	1.488	−1.765	0.155	1.118	0.299
	0.1				−0.310	1.848	−2.390	0.040	1.215	0.274
0.2	0.7	−0.075	0.263	0.167	−0.103	0.161	−1.040	0.669	RW	0.178
	0.5				−0.094	0.192	−1.120	0.458	RW	0.175
	0.3				−0.083	0.234	−1.305	0.260	RW	0.170
	0.1				−0.065	0.303	−1.880	0.079	1.513	0.163

For our initial data, the difference in volume concentration on the CD is not large: $\Delta m = 0.2$. Behind the incident SW moving to the CD, the volume concentration of the heavy component increases ($t = 20$), i.e., this phase is compacted. Reaching the CD, the incident SW interacts with the CD, and the CD starts to move in the direction of SW motion with a constant velocity behind the transient SW. The value of m_2 increases both in the transient and incident SW. Behind the transient SW, there follows the CD separating regions with different volume concentrations behind the transient and reflected waves; the difference in volume concentrations is 0.299 (Table 1). Thus, the difference increases by 50%. The value of m_2 behind the reflected SW increases.

It should be noted that stabilization of the reflected dispersed SW requires a longer time than stabilization of the transient SW.

We study the case where the volume concentration of the phases behind the combined boundary is $m_{10}^{**} = 0.5$. Interacting with the CD, the incident frozen-dispersed SW with an internal SW in the light phase and a continuous flow in the heavy phase decomposes into two dispersed shock waves. The first SW propagates in the same direction as the incident SW but has a higher velocity $D_{\text{tr}} = -1.645$. The second SW moves with a velocity $D_{\text{r}} = 0.415$ in the opposite direction with respect to the incident SW. The shape of the pressure profiles of the transient and reflected SW is monotonically increasing.

In studying the distributions of the mean densities of the light component at different times, we can note that there is a small region with elevated density and volume concentration of the carrier phase behind the CD front. The nature of this phenomenon is similar to that considered in [10] for the case of SW reflection from a rigid wall. The maximum density of the light component is 2.294, which is greater than the final equilibrium value by 0.031, and the maximum volume concentration is 0.778 (the final equilibrium value is 0.768). Correspondingly, the volume concentration and density of particles are lower than in the final equilibrium state. Thus, an increase in the difference in volume concentration ahead of the CD and behind it leads to the emergence of a moving layer with increased (decreased) volume concentration and density of the light (heavy) component.

With further decrease in concentration of the first phase ($m_{10}^{**} = 0.3$ and $\Delta m = 0.6$), the reflected SW (which is now of the frozen-dispersed type) becomes stronger, and the transient SW of the dispersed type becomes weaker. After stabilization, the transient and reflected shock waves propagate with velocities corresponding to those determined analytically in the equilibrium approximation in [1]. The CD velocity determined by an unsteady numerical calculation also corresponds to the CD velocity obtained analytically in the equilibrium approximation. The velocities of the transient and reflected shock waves become greater than in the case of $m_{10}^{**} = 0.5$ or $m_{10}^{**} = 0.7$ (Table 1). The pressure profile for the heavy component in the reflected SW becomes nonmonotonic, and a local maximum $P_2^{\max} = 2.280$ arises. This value of $P_2^{\max}$ is greater than the final equilibrium value equal to 2.253 but smaller than $P_2^{\max} = 2.525$ reached in the incident SW. The profiles of densities and volume concentrations of the phases are similar to those considered previously for $m_{10}^{**} = 0.5$ with the only difference that the amplitude of the reflected SW and CD increases, whereas the amplitude of the transient SW decreases. The amplitude of the peak (valley) of density and volume concentration of the light (heavy) phase also increases.

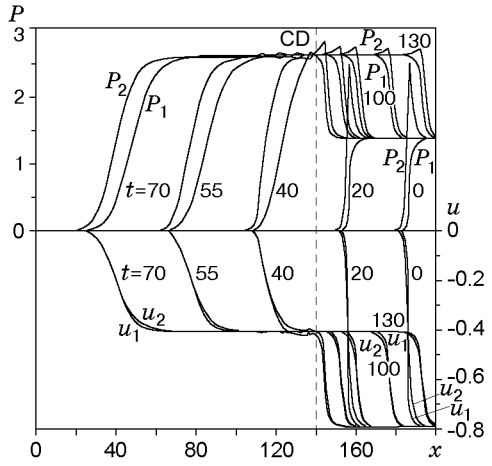

Fig. 2. Distributions of velocities and pressures of the components of the mixture for $D = -1.5$, $m_{10}^{*} = 0.9$, and $m_{10}^{**} = 0.1$.

For $m_{10}^{**} = 0.1$, the transient SW is dispersed, and the reflected SW is frozen-dispersed (Fig. 2). The velocity of the transient SW is greater than the velocity of the incident SW. Note, the velocity of transient shock waves increases with decreasing m_{10}^{**}. The reason is the increase in density of the mixture behind the CD. For example, for $m_{10}^{**} = 0.7$, 0.5, 0.3, and 0.1, the velocities of the transient SW are $D_{\rm tr} = -1.55$, -1.645, -1.92, and -2.533, and the densities are $\rho_0^{**} = 1.495$, 1.825, 2.155, and 2.485, respectively. The pressure in the transient SW increases monotonically in both components; in the reflected SW, the pressure of the light component increases jumplike in the internal SW, and the pressure of the heavy component increases up to $P_2^{\max} = 2.760$ and then decreases to the final value $P_{\rm r} = 2.658$. Comparing the case considered here with that for $m_{10}^{**} = 0.3$, we note that the relative amplitude of the pressure peak in the heavy phase increases: $\Delta P_2 = P_2^{\max} - P_{\rm r} = 0.105$ and $\Delta P_2 = 0.026$ or $\Delta \bar{P}_2 = (P_2^{\max} - P_{\rm r})/P_{\rm r} = 3.97\%$ and $\Delta \bar{P}_2 = 1.16\%$, respectively. In Fig. 2, there is a small region with different pressures of the phases, which is located between the sections with steady values of phase pressures behind the transient and reflected shock waves. The position of the region of pressure nonequilibrium coincides with the CD boundary. Thus, the theory of the CD [2] is confirmed, which proves the existence of a pressure difference on the CD. The behavior of volume concentrations and densities of the phases is similar to that for $m_{10}^{**} = 0.3$.

Variation of Porosity of the Mixture ahead of the CD. We study the interaction of an incident SW of the dispersed type propagating with a velocity $D = -1.5$ over a mixture with $m_{10}^{*} = 0.5$ and a CD behind which the value of m_{10}^{**} varies discretely from 0.1 to 0.9. Upon interaction with a denser medium ($m_{10}^{**} = 0.1$, 0.3, and 0.4), the incident SW decomposes into a reflected SW and a transient SW of the dispersed type. The velocity and pressure profiles of the components are monotonic both for the incident SW and for the reflected and refracted shock waves. As it could be expected, the velocity of the transient SW decreases with decreasing amplitude of the incident SW from 0.792 for $m_{10}^{*} = 0.9$ to 0.452 for $m_{10}^{*} = 0.5$, and the velocity of the reflected SW increases. The velocity of the CD boundary and the pressure on the CD decrease with decreasing m_{10}^{*} (see Table 1).

With increasing volume concentration of the light component behind the CD boundary ($m_{10}^{**} = 0.6$, 0.7, and 0.9), the flow pattern changes, since the density of the mixture behind the CD is lower than the density ahead of the CD. Figure 3 shows the pressure distribution before and after interaction of the dispersed SW and the CD with $m_{10}^{**} = 0.9$ behind the latter. It follows from Fig. 3 that the incident dispersed SW propagating over a dense mixture ($t = 100$ and 200) approaches the boundary of porosity discontinuity ($t = 250$) and interacts with a less dense medium. As a result of interaction, the incident SW decomposes into a transient frozen-dispersed SW and a reflected rarefaction wave. The transient frozen-dispersed SW is characterized by monotonically decreasing velocity profiles and monotonically increasing pressures of the components of the mixture, for example, for $m_{10}^{**} = 0.6$ or by a monotonically increasing pressure profile in the light component and a pressure maximum in the heavy component: $P_2^{\max} = 1.048$ and 1.361 for $m_{10}^{**} = 0.7$ and 0.9, respectively. These values of $P_2^{\max}$ are greater than the final equilibrium pressure on the CD $P_{\rm CD} = 1.035$ and 0.859, respectively. Note that the value of the local pressure maximum in the second component $P_2^{\max}$ for $m_{10}^{**} = 0.9$ is greater than the final equilibrium pressure behind the

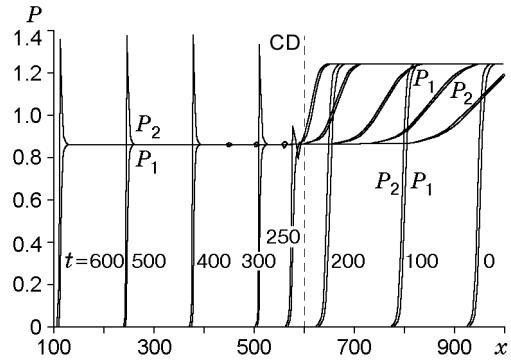

Fig. 3. Interaction of the incident dispersed SW ($D = -1.5$ and $m_{10}^{*} = 0.5$) and the CD ($m_{10}^{**} = 0.9$).

TABLE 2

Parameters of the Mixture Established after Interaction of the Incident SW ($D = -2.5$) and the CD

m_{10}^{*}	m_{10}^{**}	u_{fin}	P_{fin}	$m_{1,\text{fin}}$	u_{CD}	P_{CD}	D_{tr}	$m_{1,\text{tr}}$	D_{r}	$m_{1,\text{r}}$
0.9	0.7	−1.963	5.719	0.624	−1.703	7.840	−2.450	0.260	−0.472	0.575
	0.5				−1.558	9.260	−2.630	0.119	−0.374	0.549
	0.3				−1.440	10.526	−2.947	0.051	−0.294	0.529
	0.1				−1.328	11.586	−3.400	0.013	−0.214	0.511
0.5	0.9	−1.325	6.047	0.151	−1.583	3.981	−2.155	0.678	RW	0.190
	0.7				−1.453	4.974	−2.294	0.321	RW	0.168
	0.6				−1.389	5.498	−2.381	0.221	RW	0.159
	0.4				−1.261	6.625	−2.642	0.100	0.998	0.144
	0.3				−1.197	7.236	−2.813	0.064	1.050	0.137
	0.1				−1.063	8.575	−3.238	0.015	1.163	0.124
0.1	0.7	−0.375	2.332	0.035	−0.540	1.131	−1.402	0.534	RW	0.052
	0.5				−0.499	1.414	−1.555	0.305	RW	0.046
	0.3				−0.447	1.786	−1.855	0.142	RW	0.041

incident SW ($P_{\text{fin}} = 1.236$). Figure 3 shows the reconstruction of the incident dispersed SW into a frozen-dispersed SW upon passing into a less dense medium ($m_{10}^{**} = 0.9$). Note, the velocity of the transient SW is smaller than the velocity of the incident SW and decreases with increasing m_{10}^{**}.

A similar flow pattern is observed when a weak dispersed SW ($D = -1.5$ and $m_{10}^{*} = 0.2$) passes through the CD. In this case, the CD velocity has the lowest value (see Table 1).

Effect of Velocity of the Incident SW. An increase in velocity of the incident SW (up to $D = -2.5$) propagating over a medium with $m_{10}^{*} = 0.1$ and 0.5 and interacting with a less dense medium ($m_{10}^{**} > m_{10}^{*}$) leads to an increase in velocities of the CD and transient SW, and also to an increase in pressure on the CD and in the final equilibrium state (Table 2). In the case of interaction of the incident SW with a denser medium, i.e., for $m_{10}^{**} < m_{10}^{*}$, it decomposes into a transient SW with similar velocity and pressure profiles of the components (the velocity amplitude decreases, and the pressure amplitude increases with increasing density of the medium on the CD) and a reflected SW of the dispersed type with monotonic velocity and pressure profiles. Note, the width of the reflected SW increases with increasing m_{10}^{**}.

Thus, an increase in velocity yields results similar to those obtained for $D = -1.5$. Only the propagation velocities and amplitudes of SW formed are different.

We consider in more detail the case for $D = -2.5$ and $m_{10}^{*} = 0.9$. In this case, an incident SW of the frozen-dispersed type interacts with a denser medium in which the volume concentration of the first phase m_{10}^{**} varies discretely from 0.1 to 0.7 with a step of 0.2. In all cases, the incident SW decomposes into transient and reflected shock waves. The special feature of the variant considered is the fact that the reflected SW moves behind the CD and transient SW from the viewpoint of a motionless observer. The reason is that the reflected SW is entrained by the flow formed behind the front of the incident SW.

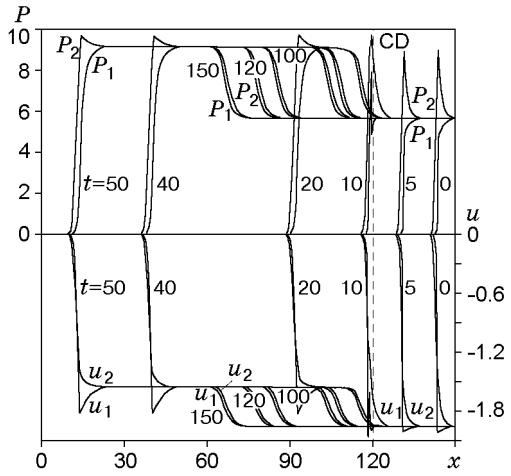

Fig. 4. Velocity and pressure distributions of the components of the mixture upon interaction of the frozen-dispersed SW ($D = -2.5$ and $m_{10}^{*} = 0.9$) and the CD ($m_{10}^{**} = 0.5$).

TABLE 3

Parameters of the Mixture Established after Interaction of the Incident SW ($D = -3.3$) and the CD

m_{10}^{*}	m_{10}^{**}	u_{fin}	P_{fin}	$m_{1,\text{fin}}$	u_{CD}	P_{CD}	D_{tr}	$m_{1,\text{tr}}$	D_{r}	$m_{1,\text{r}}$
0.9	0.7	−2.823	10.852	0.525	−2.502	15.159	−3.230	0.192	−1.145	0.475
	0.5				−2.320	18.123	−3.360	0.085	−1.035	0.453
	0.3				−2.189	20.503	−3.590	0.036	−0.948	0.437
	0.1				−2.099	22.236	−3.970	0.009	−0.887	0.427
0.4	0.9	−1.903	12.497	0.070	−2.330	7.716	−2.840	0.578	RW	0.092
	0.7				−2.150	9.604	−2.980	0.236	RW	0.081
	0.5				−1.983	11.523	−3.200	0.106	RW	0.073
	0.3				−1.825	13.483	−3.440	0.044	—	0.067
	0.1				−1.674	15.495	−3.720	0.011	0.867	0.062
0.1	0.9	−1.128	9.246	0.015	−1.634	4.216	−2.200	0.671	RW	0.025
	0.7				−1.512	5.318	−2.350	0.311	RW	0.021
	0.5				−1.390	6.513	−2.575	0.145	RW	0.018
	0.3				−1.262	7.814	−2.875	0.061	RW	0.016

Figure 4 shows the interaction of the incident SW ($D = -2.5$ and $m_{10}^{*} = 0.9$) and the CD with $m_{10}^{**} = 0.5$ in the mixture behind the CD boundary. The cross section $x = 120$ contains the CD boundary separating two regions: $x \in [0, 120)$ where $m_{10} = m_{10}^{**} = 0.5$ and $x \in [120, 150]$ where $m_{10} = m_{10}^{*} = 0.9$. It follows from Fig. 4 that the prescribed SW configuration ($t = 0$) propagates steadily over the mixture ahead of the CD at the time $t = 5$. At $t = 10$, it interacts with the CD and decomposes into a transient SW of the frozen-dispersed type and a reflected SW of the dispersed type. At the time $t = 20$, the front part of the transient SW may be considered to be formed, whereas the zone of velocity relaxation up to the equilibrium value reached on the CD (u_{CD}) may be considered to become steady only at the time $t = 30$. At later times $t = 40$ and 50, the completely formed transient SW propagates steadily over the mixture with $m_{10}^{**} = 0.5$ and a constant velocity $D_{\text{tr}} = -2.63$. The reflected SW is formed immediately after interaction of the incident SW and CD. At the time $t = 20$, its main profile is formed, and the process of SW formation may be considered to be completed at $t = 30$. At $t = 40$–150, the reflected SW of the dispersed type propagates steadily in the direction of the transient SW. It should be noted that the direction of motion of the reflected SW does not change, since the reflected SW is entrained by the flow arising behind the incident SW front.

The change in m_{10}^{**} from 0.1 to 0.7 decreases the difference in velocities D_{tr} and D_{r} ($|\Delta D| = |D_{\text{tr}} - D_{\text{r}}|$). For example, we have $|\Delta D| = 3.186$ for $m_{10}^{**} = 0.1$, $|\Delta D| = 2.653$ for $m_{10}^{**} = 0.3$, and $|\Delta D| = 1.978$ for $m_{10}^{**} = 0.7$.

We consider the case where the velocity of the incident SW is greater than the velocity of sound in pure materials ($a_i < D = -3.3$). For $m_{10}^{*} = 0.1$, the incident SW is an SW of the dispersed-frozen type. In the case of

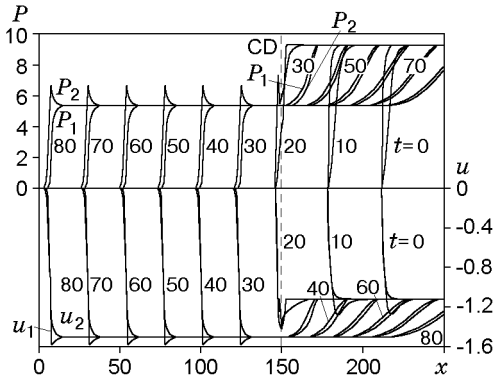

Fig. 5. Interaction of the dispersed-frozen SW ($D = -3.3$ and $m_{10}^{*} = 0.1$) and the CD ($m_{10}^{**} = 0.7$).

TABLE 4

Relative Change in the Distance between the Transient and Reflected SW for $m_{10}^{*} = 0.9$

m_{10}^{**}	$(D_{\rm tr} - D_{\rm r})/D_{\rm tr}$		
	$D = -1.5$	$D = -2.5$	$D = -3.3$
0.1	1.210	0.937	0.777
0.3	1.245	0.900	0.736
0.5	1.252	0.858	0.692
0.7	—	0.807	0.646

interaction of such an SW with a less dense medium ($m_{10}^{**} = 0.3$, 0.5, 0.7, and 0.9), the incident SW decomposes into a transient SW and a rarefaction wave. The amplitude of velocity of the transient SW is greater than that of the incident SW (Table 3). With increasing m_{10}^{**}, the increases in velocity amplitude are 11.9, 23.2, 34.0, and 44.9% for the corresponding values of m_{10}^{**}, and the amplitude of pressure in the transient SW decreases by 15.5, 29.6, 42.5, and 54.4%, respectively. A comparison of velocity and pressure variations with similar data for $D = -2.5$ shows that the relative increase in velocity and pressure amplitude decreases almost by 10% with increasing velocity of the incident SW. For all values of m_{10}^{**} considered, the velocity of the transient SW is smaller, and its type differs from the type of the incident SW. In particular, when the incident SW enters a mixture with $m_{10}^{**} = 0.3$ and 0.5, the wave changes to the dispersed type with a nonmonotonic velocity profile in the first component and a nonmonotonic pressure profile in the second component. For $m_{10}^{**} = 0.7$ and 0.9, the transient SW is of the frozen-dispersed type with an internal discontinuity in the light component.

Figure 5 shows the pressure and velocity distributions of the components of the mixture upon interaction of the incident SW ($D = -3.3$ and $m_{10}^{*} = 0.1$) and the CD with $m_{10}^{**} = 0.7$ behind it. The initial position of the CD boundary corresponds to the coordinate $x = 150$ (shown by the dashed vertical line in Fig. 5). The incident dispersed-frozen SW propagates steadily over the mixture ($t = 10$), interacts with the CD boundary ($t = 20$), and decomposes into a frozen-dispersed SW moving over the mixture at $t = 30$–80 and a reflected rarefaction wave (RW).

For $m_{10}^{*} = 0.9$, the incident SW is a frozen-type SW with a two-front configuration. Upon interaction of the incident SW and the CD behind which $m_{10}^{**} = 0.1$, 0.3, 0.5, and 0.7, it decomposes into transient and reflected shock waves. The reflected SW moves in the same direction as the transient SW.

The calculated relative changes in the distance between the transient and reflected SW $(D_{\rm tr} - D_{\rm r})/D_{\rm tr}$ for $m_{10}^{*} = 0.9$ are listed in Table 4 for different velocities of the incident SW and identical values of m_{10}^{**}. It follows from Table 4 that the distance between the transient and reflected SW increases with increasing m_{10}^{**} for $D = -1.5$ and decreases for $D = -2.5$ and -3.3, since the direction of the reflected SW changes.

Interaction of the Rarefaction Wave and the CD. The rarefaction wave was initiated from discontinuous stepwise initial data; $D = -1.2$ and $m_{10}^{*} = 0.2$. As is shown in [11], the fore RW front propagates with a variable velocity changing from the frozen ($C_{\rm f}$) to the equilibrium ($C_{\rm e}$) velocity of sound, and the aft front propagates with the least velocity of sound in the mixture, i.e., with the velocity of sound of the light component a_1. In the case

of RW interaction with a denser medium behind the CD boundary ($m_{10}^{**} = 0.1$), the transient and reflected waves are rarefaction waves. In the transient RW, the velocity changes from 0 to $u_{\rm CD} = 0.086$, the pressure changes from 0 to $P_{\rm CD} = -0.317$, and the volume concentration of the light component changes from 0.1 to $m_{1,\rm tr} = 0.138$. The reflected RW propagates in the mixture with parameters established behind the transient RW ($u_{\rm fin} = 0.102$, $P_{\rm fin} = -0.280$, and $m_{1,\rm fin} = 0.256$). Equilibrium parameters established behind the reflected RW correspond to parameters ahead of the moving CD ($P_{\rm CD}$, $u_{\rm CD}$, and $m_{1,\rm r} = 0.265$). In contrast to SW–CD interaction, upon RW–CD interaction, the latter moves with a constant velocity $u_{\rm CD}$ in the opposite direction with respect to the transient RW or in the direction of the reflected RW.

When the incident RW interacts with a less dense medium ($m_{10}^{**} > m_{10}^{*}$), it decomposes into a transient RW with increasing velocities and decreasing pressures of the components of the mixture and a reflected wave with increasing velocities and pressures of the components, which compresses the mixture formed behind the incident RW. With increasing m_{10}^{**} ($m_{10}^{**} = 0.3$, 0.5, 0.7, and 0.9), the velocity behind the transient RW increases (0.113, 0.129, 0.141, and 0.151, respectively), and its propagation velocity decreases; the pressure amplitude of the transient RW also decreases (-0.254, -0.215, -0.185, and -0.157, respectively). In the reflected compression wave, with increasing m_{10}^{**} ($m_{10}^{**} = 0.3$, 0.5, 0.7, and 0.9), the velocity amplitude increases (0.011, 0.027, 0.039, and 0.049, respectively) and the pressure amplitude increases (0.026, 0.065, 0.095, and 0.123, respectively).

The difference in volume concentration of the light (heavy) component at the CD boundary is not constant as the RW passes through the CD. For example, for $m_{10}^{**} = 0.1$, the difference is $\Delta m_0 = 0.1$ before RW–CD interaction and $\Delta m_{\rm fin} = 0.127$ after interaction, i.e., it increases by 27%; the increase is only 13% for $m_{10}^{**} = 0.3$, 6% for $m_{10}^{**} = 0.5$, and 1.4% for $m_{10}^{**} = 0.7$; for $m_{10}^{**} = 0.9$, the difference decreases by 2%.

The types of incident, transient, and reflected waves for various initial parameters of the mixture are listed in Table 5.

Comparison of Analytical and Numerical Results. Tables 1–3 give the flow parameters in equilibrium states behind the incident SW ($u_{\rm fin}$, $P_{\rm fin}$, and $m_{1,\rm fin}$) and also the parameters established after SW–CD interaction ($D_{\rm tr}$, $D_{\rm r}$, $u_{\rm CD}$, $P_{\rm CD}$, $m_{1,\rm tr}$, and $m_{1,\rm r}$) for various ratios of initial volume concentrations on the CD and incident SW velocities. An analysis of the data in Tables 1–3 allows us to make the following conclusions.

— With increasing m_{10}^{**}, the absolute value of velocity of the transient SW, the pressure on the CD, and the velocity of the reflected SW and CD boundary decrease due to the decrease in density of the mixture behind the CD.

— With increasing m_{10}^{*}, the pressure on the CD and the velocity of the transient SW and CD increase, and the velocity of the reflected SW decreases, which is caused by the increase in velocity and pressure amplitudes in the incident SW.

— An increase in velocity of the incident SW leads to a natural growth in the velocity of the CD boundary and the pressure on the CD.

The special feature of the process considered is the different character of variation of velocity of the reflected SW. As it follows from Tables 1–3, with increasing absolute velocity of the incident SW, the velocity of the reflected SW moving in the opposite direction with respect to the initial position of the CD boundary ($D_{\rm r} > 0$) gradually decreases and vanishes ($D_{\rm r} = 0$) at a certain value $D = D^*$. A further increase in velocity ($|D| > |D^*|$) leads to entrainment of the reflected SW ($D_{\rm r} < 0$), i.e., it moves in the direction of the transient SW and CD boundary.

A comparison of parameters established after interaction of the incident SW and CD, which were obtained by numerical calculations of the unsteady problem (see Tables 1–3), and results obtained in the equilibrium approximation (see Tables 1–3 in [1]) revealed some regular features. In particular, the difference between numerical and analytical calculations increases in the following cases:

— with increasing volume concentration of the light component m_{10}^{*} ahead of the CD boundary, i.e., with increasing velocity and pressure amplitudes in the incident SW;

— with increasing volume concentration of the light component behind the CD boundary;

— with increasing velocity of the incident SW.

Note that the difference between the equilibrium parameters obtained by analytical methods and numerical results obtained by the TVD difference scheme is smaller than in the case of using the modified method of "coarse particles."

TABLE 5

Wave types

m_{10}^{*}	m_{10}^{**}	Incident	Transient	Reflected
		$D = -1.2$		
0.2	0.1	RW	RW	RW
	0.3	RW	RW	CW
	0.5	RW	RW	CW
	0.7	RW	RW	CW
	0.9	RW	RW	CW
		$D = -1.5$		
0.2	0.1	DSW	DSW	DSW
	0.3	DSW	DSW	RW
	0.5	DSW	DSW	RW
	0.7	DSW	DSW	RW
0.5	0.1	DSW	DSW	DSW
	0.3	DSW	DSW	DSW
	0.4	DSW	DSW	DSW
	0.6	DSW	FDSW	RW
	0.7	DSW	FDSW	RW
	0.9	DSW	FDSW	RW
0.9	0.1	FDSW	DSW	FDSW
	0.3	FDSW	DSW	FDSW
	0.5	FDSW	DSW	DSW
	0.7	FDSW	FDSW	DSW
		$D = -3.3$		
0.1	0.3	DFSW	FDSW	RW
	0.5	DFSW	FDSW	RW
	0.7	DFSW	FDSW	RW
	0.9	DFSW	FDSW	RW
0.4	0.1	DFSW	DFSW	DSW
	0.3	DFSW	DFSW	DSW
	0.5	DFSW	DFSW	RW
	0.7	DFSW	FDSW	RW
	0.9	DFSW	FDSW	RW
0.9	0.1	FSW	DFSW	DSW
	0.3	FSW	DFSW	DSW
	0.5	FSW	FSW	DSW
	0.7	FSW	FSW	DSW

Notes. The following wave types are obtained: rarefaction wave (RW), compression wave (CW), dispersed shock wave (DSW), frozen-dispersed shock wave (FDSW), dispersed-frozen shock wave (DFSW), and frozen shock wave with a two-front configuration (FSW).

CONCLUSIONS

Numerical simulation of wave interaction with the CD allows us to make the following conclusions.

Interacting with the CD, incident shock waves of various types decompose into shock waves whose type depends on the relationship of the components in the initial state of the mixture. Special features of the behavior of parameters depending on the incident SW velocity are revealed.

Upon interaction with the CD, rarefaction waves decompose into rarefaction waves or compression waves, depending on the initial concentrations of the components in the mixture.

REFERENCES

1. A. A. Zhilin and A. V. Fedorov, "Interaction of shock waves with a combined discontinuity in two-phase media. 1. Equilibrium approximation," *J. Appl. Mech. Tech. Phys.*, **43**, No. 3, 380–390 (2002).
2. A. V. Fedorov and V. M. Fomin, "Theory of a combined discontinuity in gas mixtures," in: *Physical Gas Dynamics of Reacting Media* [in Russian], Nauka, Novosibirsk (1990), pp. 128–134.
3. A. A. Gubaidullin, A. I. Ivandaev, and R. I. Nigmatulin, "Modified method of 'coarse particles' for calculation of unsteady wave processes in multiphase disperse media," *Zh. Vychisl. Mat. Mat. Fiz.*, **17**, No. 6, 1531–1544 (1977).
4. A. A. Zhilin and A. V. Fedorov, "Propagation of shock waves in a two-phase mixture with different pressures of the components," *J. Appl. Mech. Tech. Phys.*, **40**, No. 1, 46–53 (1999).
5. R. P. Fedorenko, "Application of high-accuracy difference schemes for the numerical solution of hyperbolic equations," *Zh. Vychisl. Mat. Mat. Fiz.*, **2**, No. 6, 1122–1128 (1962).
6. G. A. Ruev, B. L. Rozhdestvenskii, V. M. Fomin, and N. N. Yanenko, "Conservation laws in systems of equations of two-phase media," *Dokl. Akad. Nauk SSSR*, **254**, No. 2, 288–293 (1980).
7. A. Harten, "High resolution schemes for hyperbolic conservation laws," *J. Comput. Phys.*, **49**, No. 3, 357–393 (1983).
8. A. A. Zhilin, "Structure and propagation of shock waves in two-component mixtures," Candidate's Dissertation in Phys.-Math. Sci., Novosibirsk (1999).
9. A. A. Zhilin, "Application of a TVD scheme for calculating two-phase flows with different velocities and pressures of the components," in: *Proc. Conf. of Young Scientists Devoted to the 10th Anniversary of the Institute of Computational Technologies of the Siberian Division of the Russian Academy of Sciences* (Novosibirsk, Dec. 25–26, 2000), Vol. 2, Inst. Comput. Technol., Novosibirsk (2001), pp. 61–65.
10. A. A. Zhilin and A. V. Fedorov, "Reflection of shock waves from a solid boundary in a mixture of condensed materials. 2. Nonequilibrium approximation," *J. Appl. Mech. Tech. Phys.*, **40**, No. 6, 995–1001 (1999).
11. A. A. Zhilin and A. V. Fedorov, "Reflection of a shock wave from a rigid wall in a mixture of a liquid metal and solid particles," *Combust. Expl. Shock Waves*, **36**, No. 4, 506–515 (2000).